

# Kinematic and Unsteady Aerodynamic Study on Bi- and Quad-Wing Ornithopter

(Received: March 17, 2014. Revised: April 28, 2015. Accepted: June 23, 2016)

H.DJOJODIHARDJO<sup>1</sup>  
A.S.S.RAMLI<sup>1</sup>  
M.A.A.BARI<sup>2</sup>

## Abstract

The potential of Flapping Wing Micro Air Vehicles (MAVs) for sensing and information gathering relevant for environmental and disaster monitoring and security surveillance leads to the identification and modeling the salient features and functional significance of the various components in the flying reasonably sized biosystems. The dynamics, kinematics and aerodynamics of their wing systems and the production of mechanical power output for lift and thrust will be synthesized following a simplified and generic, but meticulous, model for a flapping wing ornithopter. Basic unsteady aerodynamic approach incorporating viscous effect and leading-edge suction is utilized. The first part of the study is focused on a bi-wing ornithopter. Later, parametric study is carried out to obtain the lift and thrust physical characteristics in a complete cycle for evaluating the plausibility of the aerodynamic model and for the synthesis of an ornithopter model with simplified mechanism. Further analysis is carried out by differentiating the pitching and flapping motion phase-lag and studying its respective contribution to the flight forces. A similar procedure is then applied to flapping quad-wing ornithopter model. Results are discussed in comparison with various selected simple models in the literature, with a view to develop a practical ornithopter model.

## 1 Introduction

Motivated by flying biosystems, flight engineering has been initiated since hundreds of years ago and has gradually grown from the time of Leonardo Da Vinci to Otto Lilienthal's gliders, to modern aircraft technologies and present flapping flight research. Recent interest in the latter has grown significantly particularly for small flight vehicles (or Micro-Air-Vehicles) with very small payload carrying capabilities to allow remote sensing missions in hazardous as well as confined areas. Some of these vehicles may have a typical wingspan of 15 cm, with a weight restriction of less than 100 g [1]. Perhaps the most comprehensive account of insect flight or entomopter to date is given by Weis-Fogh [2], Ellington [3-5], Shyy et al [6,7], Dickinson et al [8], bikowski [9] and Ansari et al [10], while one of the first successful attempts to develop birdlike flapping flight was made by DeLaurier [11]. In a recent paper, Wang [12, 13] has elaborated the peculiar nature of insects hovering, which has been efficiently acquired not by the dominant aerodynamic lift, but by the drag in a paddling like motion.

Although our interest in developing a mathematical and experimental model is on more or less rigid bi- and quad- wing ornithopter, it should also take note on other relevant lightweight, flexible wings characteristics of insects and hummingbirds, that undergo large deformations while flapping, which can increase the lift of flapping wings (Rosenfeld [14]), as applicable.

In the past, flapping wing designs have been created with varied success, for forward or hover mode, but not both, based on observations of hummingbirds and bats (Nicholson et al [15]). According to Maybury and Lehmann [16], the dragonfly has the capability to shift flight modes simply by varying the phase lag between its fore and hind wings. With that observation, a quad-winged flapping

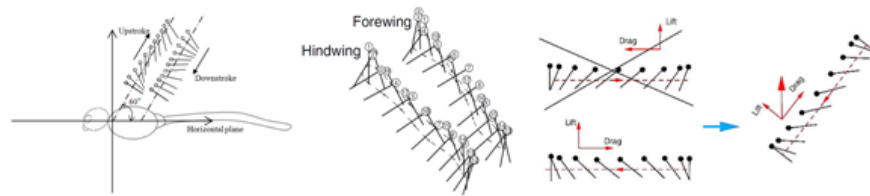
<sup>1</sup> Department of Aerospace Engineering, Faculty of Engineering, Universiti Putra Malaysia, 43400 UPM Serdang, Selangor, Malaysia

<sup>2</sup> Aerodynamics & Flight Mechanics Research Group, University of Southampton, Southampton SO17 1BJ, UK.

**Figure 1:** a. Pterosaur [19]; b. Soaring eagle c. A dragonfly exhibiting its wing geometry and structural detail.



**Figure 2:** (a) and (b) Upstroke and downstroke motion of dragonfly (Adapted from [20]); (c) Saving power by eliminating a half stroke in normal hovering [12, 13].



system could be conceived as the simplest mechanism that has the capabilities to shift between flight modes [17]. In one of the recent works in developing quad flapping wing micro air vehicle, Ratti [17] has theoretically shown that a flight vehicle with four flapping wings has 50% higher efficiency than that with two flapping wings. Inspired by the flight of a dragonfly, Prosser [18] analyzed, developed and demonstrated a Quad-Wing Micro Air Vehicle (QW-MAV) which can produce higher aerodynamic performance and energy efficiency, and increased payload capacity compared to a conventional flapping wing MAV (FW-MAV). In developing a generic model of flapping wing ornithopter, the bi-wing ornithopter will first be reviewed and developed, and then extended to quad-wing ornithopter. In addition, the present approach is aimed at finding the simplest ornithopter configuration which can be used as the baseline for progressive and continued development. Also, by analyzing and synthesizing simple ornithopter configuration, the latter can be built into a simple mechanized one that can be used for experimental studies and further development. For this purpose, the sequence of Figs. 1 to 3 is presented, which are ordered according to the wing structure characteristics. Fig. 1 exhibits wing geometries of a Pterosaur, an eagle and a dragonfly, which could inspire the development of the geometrical and aerodynamic modelling of an ornithopter.

The image displayed in Fig. 2 exhibit a dragonfly, which will later be imitated to take advantage of the quad-wing kinematic and aerodynamic interactions, in the effort of improving the performance of the ornithopter to be developed. Fig. 2 also schematically exhibits the flapping motion of the quad-wing dragonfly, as studied by Wang and Russell [20]. It is of interest to note that a systematic study by Wang [12, 13] shows that in the case of insects with dominant hovering movement, due to comparable lift and drag components of the aerodynamic force, the sustainment of flight is attributed to the drag, like in paddling movement. Fig. 2 (c), adapted from Wang [12, 13], shows how by eliminating a half stroke in hovering, like in dragonfly, power efficiency can be achieved.

Taha et al [21] made a thorough review of the significant work done so far in the area of flight dynamics and control of flapping-wing micro-air vehicles (MAVs), covering the flapping kinematics, the aerodynamic modeling, and the body dynamics. They identified the missing gap between hover and forward speed movement, where  $k > 0.1$ , flapping frequency  $\omega$  in the order of the body natural frequency, and relative flow angle  $\alpha > 25^\circ$  or dynamic stall, where there is dominant LEV contribution and coupling between the aerodynamic forces and the body modes.

Addressing this gap and in dealing with LEV, Taha et al [22] embarked upon a novel approach of using a state-space formulation for the aerodynamics of flapping flight by extending the Duhamel's principle in the linear unsteady flows to non-conventional lift curves to capture the LEV contribution. Their proposed model has been validated through a comparison with direct numerical simulations of Navier-Stokes on hovering insects.

Table 1: Overview of some relevant characteristics of flapping biosystems (extension based on [25] and [26]).

Items	Insects	Humming Bird	Bat	Small Birds	Large Birds	Flapping MAV	Small Low Speed Airplanes
<b>1. Types</b>	Beetles, Bumblebees, Butterflies, Dragonflies,	Amazilia	Plecotus Auritus	Sparrows, Swifts, Robins	Eagle, Hawk, Vulture, Falcon, Skua Gull	DARPA DRO [1]	Cessna 210
<b>2. Weight Typical (gf)</b> <sup>1</sup>	$25 \times 10^{-5} - 12.8$	5.1	9.0	35 - 82	952-4300	$\leq 50$	1045000
<b>3. Wing Semi-span (cm)</b> <sup>1</sup>	0.062 - 7.7	5.9	11.5	20 - 48	58-102	$< 7.5$	5600
<b>Wing-Loading (g/cm<sup>2</sup>)</b>	$10^{-3} - 10^{-1}$	0.4	0.072	0.029-0.152	0.35 - 0.67	$10^{-2} - 1$	11.18
<b>4. Typical Power (gf cm sec<sup>-1</sup> per gf)</b>	5.3 - 238	130	83	93 - 110	42 - 57	$\approx 39$	$\approx 1.3 \times 10^4$
<b>5. Dominant Wing Movement</b>	Hover	Hover and Fly	Fly	Fly	Fly	Hover and Fly	Fly
<b>6. Motion elements of Wing Kinematics</b>	Pronation & supination in stroke plane	Pronation & supination in stroke plane	Flapping and pitching	Flapping and Pitching	Flapping and Pitching	Flapping and pitching	-
<b>7. Flight Speed (m/s)</b>	1.05 - 9	15	10 - 14	6 - 10	10 - 20	3-10	99m/s (cruise at 6100 m altitude)
<b>8. Reynolds No.</b>	10-1000	7500	14000	$10^3 - 10^4$	$10^4 - 10^5$	$10^1 - 10^3$	10,000,000
<b>9. Leading Edge Vortex/LEV</b>	LEV by swept wing at $Re = 5 \times 10^3$	yes	yes	yes	yes	yes	no
<b>10. Entering its own TEV/ Wake Capture</b>	yes	yes	no	no	no	no	no
<b>11. Laminar Separation Bubble/LSB</b>	yes	yes	yes	yes	yes	yes	no
<b>12. Leading Edge Flap</b>	-	-	Has been observed on bats	-	<small>e.g. Mallard, at <math>Re = 6 \times 10^4</math> (Jones et al [27])</small> 	-	-
<b>13. Self-activated flaps at TE</b>					<small>e.g. Skua Gull [6-7]</small> 		

<sup>1</sup> Power functions of wing dimensions and flight parameters against body mass  $m$ , following Shyy [7] and Norberg [23]. The exponent of correlation is for (Mass)exponent.

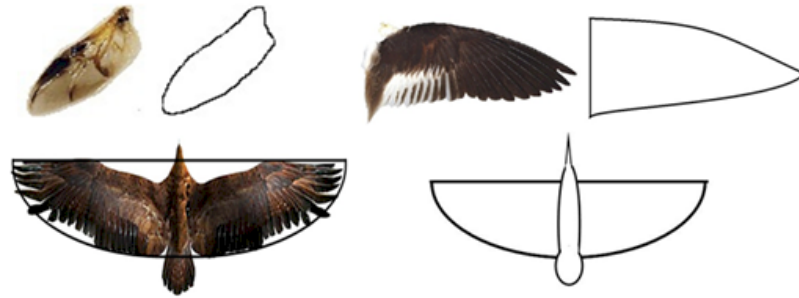
**Table 1:** Overview of some relevant characteristics of flapping biosystems (extension based on [25] and [26]).

It has also been observed that the flapping frequency tends to decrease with body mass increase [6]. In view of these findings, the classification tabulated in Table 1 could summarize some of the relevant features of flapping biosystems that may give us an overview for developing flapping ornithopter MAV. Whereas crane-flies, mosquitoes and other Nematocera as well as many larger Brachycera and Cyclorrhapha undoubtedly use normal hovering in most cases [23]. Birds habitually perform aerial maneuvers that exceed the capabilities of best anthropogenic aircraft control systems (Tedrake et al [24]). The complexity and variability of the aerodynamics during these maneuvers are difficult, with dominant flow structures (e.g., vortices) that are difficult to predict robustly from first-principles (or Navier-Stokes) models. In this conjunction, machine learning will play an important role in the control design process for responsive flight by building data-driven approximate models of the aerodynamics and by synthesizing high-performance nonlinear feedback policies based on these approximate models and trial-and-error experience.

Biosystem flapping flights are characterized by a relatively low Reynolds number, flexible wing, highly unsteady flow, laminar separation bubble, non-symmetrical upstroke and downstroke and for entomopters, the presence and significant role of the leading edge vortex, and wake vortices capture, among others.

Hence the objective of the present work are: first, to understand and mimic the kinematics and unsteady aerodynamics of biosystems that can be adopted in the present bi-wing FW-MAV and quad-wing QWMAV. Second, following our previous attempt to develop pterosaur-like ornithopter to produce lift and

**Figure 3:** A generic semi-elliptical ornithopter's wing planform with the backdrop of various wing-planform geometries: (a) a ladybug half-wing and its outline; (b) an American Avocet half-wing and its outline; (c) an eagle top view and outline and (d) the present generic wing planforms.



thrust for forward flight as a simple and workable ornithopter flight model [25, 26], the present work will simulate and analyse the kinematics and aerodynamics of bird-like rigid Bi- and Quad-Wing ornithopter.

At the present stage, which is addressed on bi-wing ornithopter mimicking bird's forward flight, the work does not incorporate leading edge vortex effects. In modeling and simulating the influence of the leading edge vortex in our future work, information gained from many recent approaches such as those of Ansari et al [10], Jane Wang [13] and Taha et al [21, 22] will be taken into consideration. A simplistic and heuristic leading edge vortex modeling which associate the shed vortices with rapid pronation of the wing is presented in a companion paper [28].

## 2 Theoretical Development of the Generic Aerodynamics of Flapping Wings

Following the frame of thought elaborated in the previous section, several generic flying biosystem wing planforms are chosen as baseline geometries for the ornithopter. Referring to the eagle wing and for convenience of baseline analysis, the semi elliptical wing (shown in Fig. 3) is selected for current study with the backdrop of various wing-planform geometries utilized by various researchers.

Analytical approaches of quasi-steady and unsteady model are carefully evaluated in the present work in order to deal with the aerodynamic problem. In agreement with the quasi-steady model, based on observation on flying birds, it can be assumed that the flapping frequencies are sufficiently slow that shed wake effects are negligible, as in pterosaur and medium- to large-sized birds. The unsteady approach attempts to model the wake like hummingbird and insects will be deferred to succeeding work. The present unsteady aerodynamic approach is synthesized using basic foundations that may exhibit the generic contributions of the motion elements of the bio-inspired bi-wing and quad-wing air vehicle characteristics.

To account for the unsteady effects, Theodorsen unsteady aerodynamics [29] and its three dimensional version by Jones [30] have been incorporated. The computation of lift and thrust generated by pitching and flapping motion of three-dimensional rigid wing is conducted in a structured approach using strip theory and Jones' modified Theodorsen approach (DeLaurier [11], Jones [30]) for a wing without camber. Furthermore, the Polhamus leading edge suction [31, 32] is also incorporated. The total lift and thrust for the wing is calculated by the summation of the contributions from each strip for a whole flapping cycle. Fully unsteady lifting-surface theory [33-36] may later be incorporated.

At the present stage, which will be assessed a posteriori based on the results, DeLaurier's [11] unsteady aerodynamics and modified strip theory approach for the flapping wing is utilized with post-stall behavior. The computational logic in the present work is summarized in the Flow-Chart exhibited in Fig. 4.

To obtain insight into the mechanism of lift and thrust generation of flapping

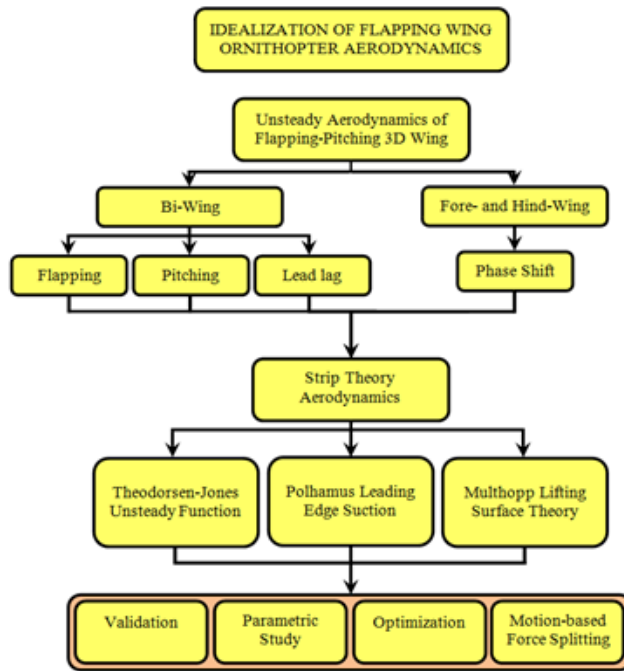


**Figure 4:** Ornithopter Flapping Wing Aerodynamics Computational Scheme.

and pitching motion, Djojodihardjo et al [37, 38] analyzed the wing flapping motion by looking into the individual contribution of the pitching, flapping and coupled pitching-flapping to the generation of the aerodynamic forces. Also the influence of the variation of the forward speed, flapping frequency and pitch-flap phase lag has been analyzed. Such approach will also be followed here through further scrutiny of the motion elements. The generic procedure is synthesized from the pitching-flapping motion of rigid wing developed by DeLaurier [11] and Harmon [39]. The flapping motion of the wing is distinguished into three distinct motions with respect to the three axes; these are: a) *Flapping*, which is up and down plunging motion of the wing; b) *Feathering* is the pitching motion of wing and can vary along the span; c) *Lead-lag*, which is in-plane lateral movement of wing, as incorporated in Fig. 5. For further reference to the present work, the lead-lag motion could be interpreted to apply to the phase lag between pitching and flapping motion, while the fore-and-aft movement can be associated with the orientation of the stroke plane. The degree of freedom of the motion is depicted in Fig. 5. The flapping angle  $\beta$  and pitching angle  $\theta$  are varied as a cosinusoidal function, given by the following equations.

$$\beta(t) = \beta_0 \cos \omega t \quad (1)$$

$$\theta(t) = \theta_0 \cos(\omega t + \phi) + \theta_{fp} \quad (2)$$

where  $\theta_0$  and  $\beta_0$  indicate maximum value for each variables,  $\phi$  is the lag between pitching and flapping angle and  $y$  is the distance along the span of the wing, and  $\theta_{fp}$  is the sum of the flapping axis angle with respect to flight velocity (incidence angle) and the mean angle of the chord line with respect to the flapping axis. A different scheme, however, can be adopted and varied for investigation purpose.

Leading edge suction is included following the analysis of Polhamus [31, 32] and DeLaurier's approximation [11]. Three dimensional effects will later be introduced by using Scherer's modified Theodorsen-Jones Lift Deficiency Factor [40], in addition to the Theodorsen unsteady aerodynamics [29] and its three dimensional version by Jones [30]. Further refinement is made to improve accuracy. Following Multhopp approach (Multhopp [41]), simplified physical approach to the general aerodynamics of arbitrary planform is adopted, i.e. a

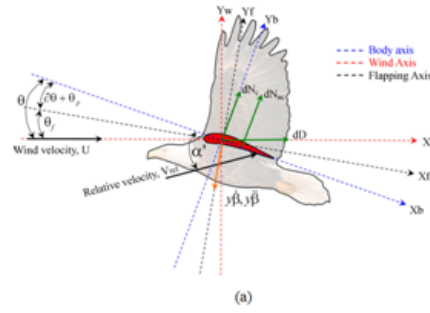


**Figure 5:** (a) Forces on section of the wing. (b),(c),(d) Flapping and pitching motion of flapping wing.

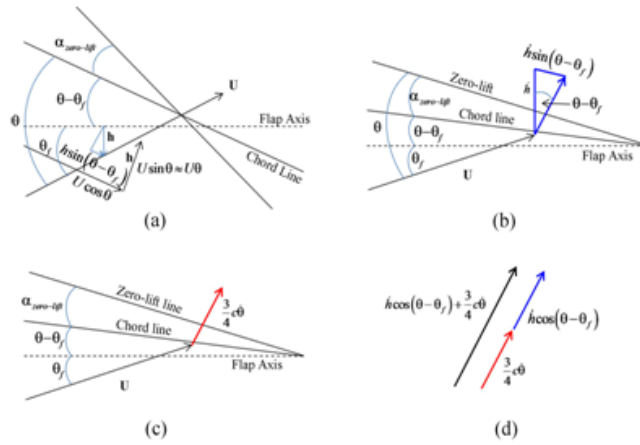
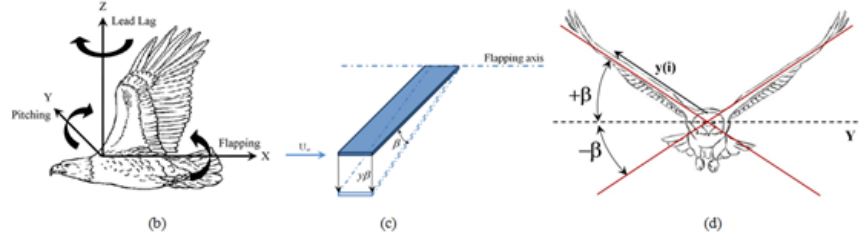


**Figure 6:** Schematic diagram of flapping and pitching components of induced velocities at chord.

lifting line in the quarter-chord line for calculating the downwash on the three-quarter-chord line for each strip.

In the present analysis no linear variation of the wing's dynamic twist is assumed for simplification and instructiveness. However, in principle, such additional requirements can easily be added due to its linearity.

The total normal force acting perpendicularly to the chord line and given by

$$dN = dN_c + dN_{nc} \quad (3)$$

The circulatory normal force for each section acts at the quarter chord and also perpendicular to the chord line is given by

$$dN_c = \frac{\rho UV}{2} C_n(y) c dy \quad (4)$$

$$dN_{nc} = \frac{\rho \pi c^2}{4} \dot{V}_{mid-chord} dy \quad (5)$$

where

$$\dot{V}_{mid-chord} = U \dot{\alpha} - \frac{1}{4} c \ddot{\theta} \quad (6)$$

Using these relationships, the relative velocity at three-quarter chord point which is used for the calculation of the aerodynamic forces can be established. The relative angle of attack at three-quarter chord,  $\alpha$ , is then given by

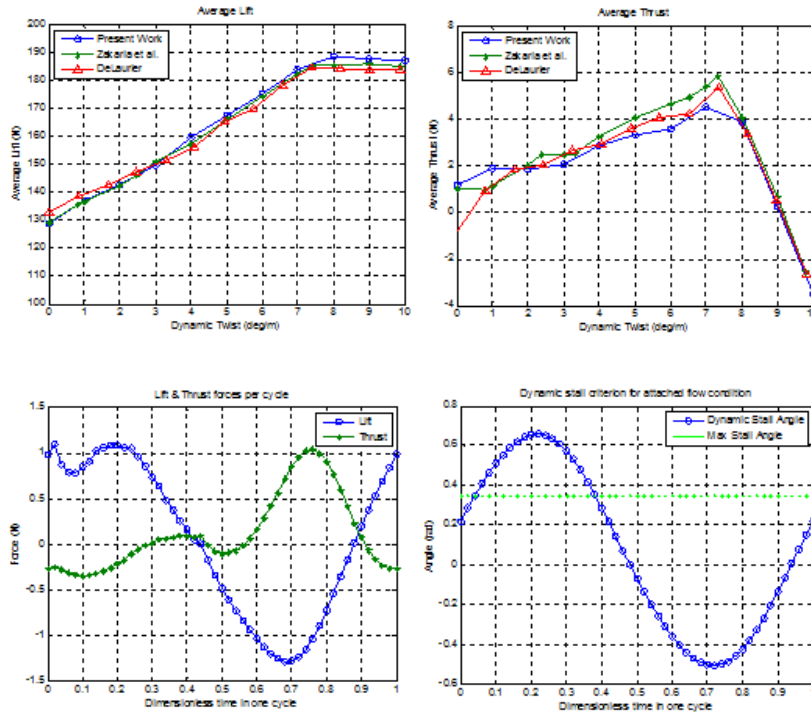


**Figure 7:** Verification of aerodynamic modelling of present work with work by Zakaria et al [46] and De Laurier [11].

**Figure 8:** Left: Lift and thrust for bi-wing ornithopter; Right: Stall angle criterion to show post-stall behavior within the present modelling.

$$\alpha = \frac{\left(\dot{h} \cos(\theta - \theta_f) + \frac{3}{4}c\dot{\theta} + U(\theta - \theta_{fp})\right)}{U} \quad (7)$$

$$\alpha = Ae^{i\omega t} \quad (8)$$

which is schematically elaborated in Fig. 6.

The modified Theodorsen Lift Deficiency function for finite aspect ratio wing is given by Jones [30]. Another derivation for unsteady forces for finite aspect ratio wing carried out by Scherer [40] arrived at a similar form to the Theodorsen two-dimensional case. It is utilized here for convenience and takes the following form

$$C(k)_{jones} = \frac{AR C(k)}{2 + AR} \quad (9)$$

where

$$C(k) = F(k) + iG(k) \quad (10)$$

$C(k)$ ,  $F(k)$  and  $G(k)$  relate to the well-known Theodorsen function [29, 30] which are functions of reduced frequency,  $k$ . Following the methodological philosophy of Theodorsen [29] and Garrick [42, 43] and the classical unsteady aerodynamics, the unsteady lift is expressed as [43]:

$$L = \pi c \rho U C(k) Q \quad (11)$$

where  $Q$  is given by  $Q = \omega e^{i\omega t}$ . Then, substitution  $Q$  into eq. (11) gives

$$L = \pi c \rho U C(k) (\omega e^{i\omega t}) \quad (12)$$

The convenience of the Complex Analysis of Theodorsen is exemplified by Garrick by associating the imaginary part of (11) and (12) with the lift [43]. The details are elaborated for the sake of completeness. The reduced frequency is defined as  $k = \frac{\omega c}{2U}$ , or  $\omega t = \frac{\omega c}{2U} \cdot \frac{2Ut}{c} = ks$ . Assuming sinusoidal motion

$$\omega e^{i\omega t} = \omega (\cos \omega t + i \sin \omega t) \quad (13)$$

or

$$\omega e^{i\omega t} = \omega (\cos ks + i \sin ks) \text{GrindEQ}_{14}(14)$$

Combining (10) and (13), one obtains:

$$L = \pi c \rho U \omega [(F(k) + iG(k)) (\cos ks + i \sin ks)] \quad (15)$$

Note that

$$|C(k)| \equiv C(k) = |F(k) + iG(k)| = \left| (F(k)^2 + G(k)^2)^{-\frac{1}{2}} \right| \quad (16)$$

where the imaginary value of Eq. (15) is the lift:

$$\alpha_{Theodorsen} = \tan^{-1} \frac{G(k)}{F(k)} \quad (17)$$

$$F(k) = |C(k)| \cos \alpha_{Theodorsen} = C(k) \cos \alpha_{Theodorsen} \quad (18)$$

$$G(k) = |C(k)| \sin \alpha_{Theodorsen} \quad (19)$$

After some algebraic manipulation, Eq. (15) reduces to

$$L = \pi c \rho U \omega .I.P \left[ \begin{array}{l} C(k) \cos(ks) \cos \alpha_{Theodorsen} - C(k) \sin(ks) \sin \alpha_{Theodorsen} \\ + i C(k) (\cos(ks) \sin \alpha_{Theodorsen} + \sin(ks) \cos \alpha_{Theodorsen}) \end{array} \right] \quad (20)$$

and the imaginary parts (I.P) of the above equation is

$$C(k) (\cos(ks) \sin \alpha_{Theodorsen} + \sin(ks) \cos \alpha_{Theodorsen}) \quad (21)$$

or

$$C(k) \sin(ks + \alpha_{Theodorsen}) \quad (22)$$

Therefore:

$$L = \pi c \rho U \omega \left[ (F(k)^2 + G(k)^2)^{-\frac{1}{2}} \sin \left( ks + \tan^{-1} \frac{G(k)}{F(k)} \right) \right] \quad (23)$$

Consistent with the strip theory, the downwash for untwisted planform wing is given by [44, 45]

$$\frac{w_o}{U} = \frac{2(\alpha_0 + \theta_{fp})}{2 + AR} \quad (24)$$

Considering all of these basic fundamentals, the relative angle of attack at three-quarter chord point  $\alpha$  is given by

$$\alpha' = \frac{AR}{(2 + AR)} \left[ F(k)\alpha + \frac{c}{2U} \frac{G(k)}{k} \dot{\alpha} \right] - \frac{w_o}{U} \quad (25)$$

which has taken into account the three dimensionality of the wing.

From Fig. 6(c), the flow velocity which include the downwash and the wing motion relative to free-stream velocity,  $V$  can be formulated as

$$V = \left[ \left( U \cos \theta - \dot{h} \sin(\theta - \theta_f) \right)^2 + \left( U (\alpha' + \theta_{fp}) - \frac{1}{2} c \dot{\theta} \right)^2 \right]^{\frac{1}{2}} \quad (26)$$

where the third and fourth terms are acting at the three-quarter chord point. The apparent mass effect for the section is perpendicular to the wing, and acts at mid chord, and can be calculated as

$$dN_{nc} = \frac{\rho\pi c^2}{4}(U\dot{\alpha} - \frac{1}{4}c\ddot{\theta})dy \quad (27)$$

The term  $U\dot{\alpha} - \frac{1}{4}c\ddot{\theta}$  is the normal velocity's time rate of change at mid-chord due to the motion of the wing.

The total chordwise force,  $dF_x$  is accumulated by three force components; these are the leading edge suction, force due to camber, and chordwise friction drag due to viscosity effect. All of these forces are acting along and parallel to the chord line.

$$dF_x = dT_s - dD_{camber} - dD_f \quad (28)$$

The leading edge suction,  $dT_s$ , following Garrick [42, 43], is given by

$$dT_s = 2\pi\eta_s \left( \alpha' + \theta_{fp} - \frac{1}{4} \frac{c\dot{\theta}}{U} \right) \frac{\rho UV}{2} cdy \quad (29)$$

while following DeLaurier [11] the chordwise force due to camber and friction is respectively given by

$$dD_{camber} = -2\pi\alpha_o(\alpha' + \theta_{fp}) \frac{\rho UV}{2} cdy \quad (30)$$

$$dD_f = \frac{1}{2}\rho V_x^2 C_{d_f} cdy \quad (31)$$

The efficiency term  $\eta_s$  is introduced for the leading edge suction  $dT_s$  to account for viscosity effects. The vertical force  $dN$  and the horizontal force  $dF_x$  at each strip  $dy$  will be resolved into those perpendicular and parallel to the free-stream velocity, respectively. The resulting vertical and horizontal components of the forces is then given by

$$dL = dN \cos \theta + dF_x \sin \theta \quad (32)$$

$$dT = dF_x \cos \theta - dN \sin \theta \quad (33)$$

To obtain a three dimensional lift for each wing, these expressions should be integrated along the span,  $b$ ; hence

$$L = \int_0^b dL dx \quad (34)$$

$$T = \int_0^b dT dx \quad (35)$$

### 3 Results

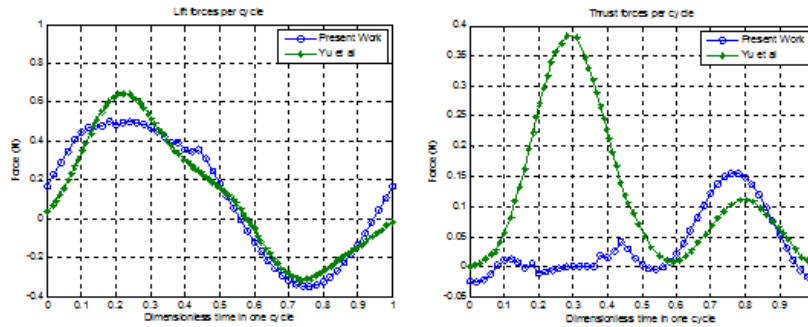
#### 3.1 Results for Bi-Wing

For later comparison with appropriate results from the literature, numerical computations are performed using the following wing geometry and parameters: the wingspan of 40cm, aspect ratio of 6.36, flapping frequency of 7Hz, total flapping angle of 60, forward speed of 6m/s, maximum pitching angle of 20, incidence angle of 6 and there is no wing dihedral angle. In the calculation, both the pitching and flapping motions are in cosine function by default, which is subject to parametric study, and the upstroke and downstroke have equal time duration. The wake capture has not been accounted for in the current

**Table 2:** Average lift and thrust of present work (bi-wing).

Av. Forces (N)	Present Work
Lift	0.0662
Thrust	0.1110

**Figure 9:** Results validation with Yu et al [47].



computational procedure. The computational scheme developed has been validated satisfactorily, starting from the verification of present work with other works by Zakaria et al [46] and DeLaurier [11] which is shown in Fig. 7, where it uses the pterosaur’s wing model.

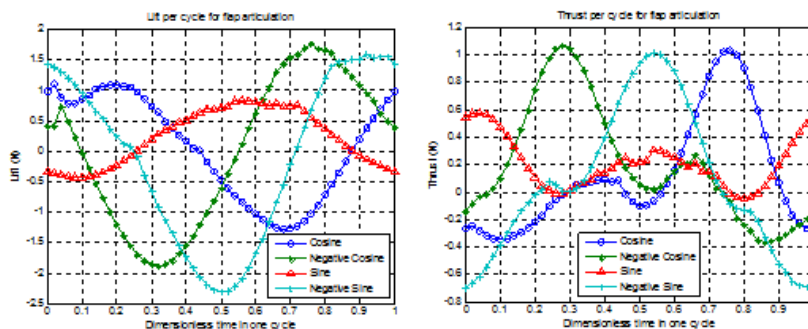
The result of bi-wing calculated using chosen wing geometry and parameters is shown qualitatively in Fig. 8 (left) and the average values of both lift and thrust forces are shown in Table 2. Also in Fig. 8 (right), the criterion for post-stall behavior is shown to emphasize that at certain angle of attack, it is exceeding the limit of maximum stall angle to enter the region of post-stall condition, eventhough the angle is only accounted for the upper (positive) limit, following DeLaurier’s assumptions in his work.

In Fig. 9, the present work uses Yu et al’s [47] parameter to produce comparable agreements qualitatively and quantitatively with the behavior of Yu et al’s [47] results. For the thrust force per cycle, during downstroke, the force is not really pronounced and low due to the stall condition, causing such trend.

### 3.1.1 Variation of oscillatory articulation of the Bi-Wing

In modeling the pitching and flapping motion of the ornithopter wing, one may learn from the biosystems as summarized in Table 1, but could also attempt to introduce variations. Based on a close observation to selected avians, such as soaring eagles, one can observe that before taking off, they expand (flap) their wings up to a maximum position and stretch their legs simultaneously. It follows, that the oscillatory motion can be modeled as a cosine function. However, many researchers did their studies with different kinematic settings for flapping and pitching motions, for example, negative sinusoidal motion. Related to this, DeLaurier introduced spanwise sinusoidal twisting for his wing model. Motivated by these meticulous observations, various possible models can be defined and utilized accordingly to account for every possible flapping kinematics. The

**Figure 10:** Lift and thrust for bi-wing ornithopter for each kinematics definition (flap articulation).



Av. Forces (N)	Present Work	Yu et al [47]
Lift	0.1243	0.121
Thrust	0.0337	0.119

**Table 3:** Average lift and thrust of present work and Yu et al's calculation [47].

Av. Forces (N)	Flap Articulation (Pitch-cosine function)			
	Cosine	- Cosine	Sine	- Sine
Lift	0.06621	0.02595	0.2193	-0.09304
Thrust	0.1110	0.1953	0.2139	0.05715

**Table 4:** Average lift and thrust (bi-wing) for flap articulation.

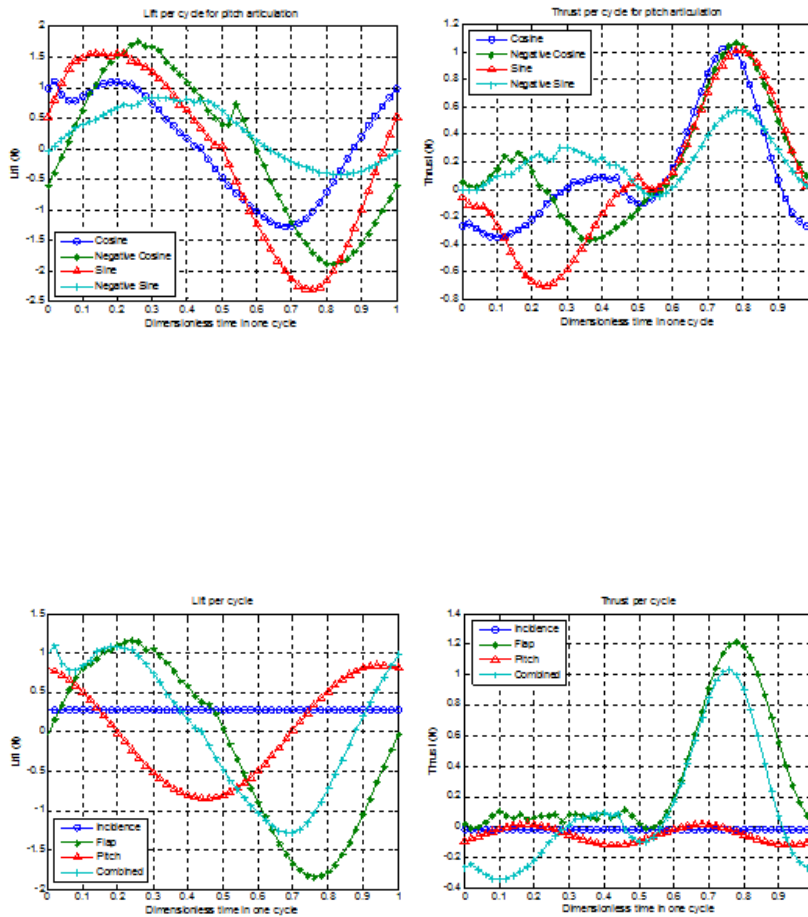


**Figure 11:** Lift and thrust for bi-wing ornithopter for each kinematics definition (pitch articulation).

**Figure 12:** The influence of individual contributions of the pitching-flapping motion and incidence angle on the flight performance.

**Table 5:** Average lift and thrust (bi-wing) for pitch articulation.

Av. Forces (N)	Pitch Articulation (Flap-cosine function)			
	Cosine	- Cosine	Sine	- Sine
<b>Lift</b>	0.06621	0.006561	-0.1094	0.2289
<b>Thrust</b>	0.1110	0.2001	0.07077	0.2062

**Table 6:** Average lift and thrust (bi-wing) for each individual contribution.

Av. Forces (N)	Individual Contribution for Bi-wing			
	Incidence only	Flap only	Pitch only	Combined
<b>Lift</b>	0.2776	-0.1864	0.01615	0.06621
<b>Thrust</b>	-0.01803	0.3123	-0.05182	0.1110

results are shown in Fig. 10 and 11, and Table 4 and 5.

What can be seen in Fig. 10 and 11 is that, in conformity with our observation and those researchers like DeLaurier [11], Fujiwara et al [48] and Chen et al [49], flapping motion should be in cosine function. Interestingly, as observed by Chen et al and assumed by DeLaurier, the pitching motion is prominent in negative sine function and exhibited by our calculation. Table 5 lists the average lift and thrust for various pitch articulation. Judging from these results, at least within the assumptions adopted in the present work, one can obtain an impression, which combination of cosine-flap and negative sine-pitch produces the highest value of lift and thrust forces. These results exemplify that the flapping kinematics can produce significant aerodynamics forces and the sensitivity of the lift and thrust produced to the oscillatory articulation could be utilized for tailoring or optimization purposes. Further investigation is currently in progress.

### 3.1.2 Component-wise Forces for Bi-Wing

Another study is carried out to investigate the influence of individual contributions of the pitching-flapping on the flight performance. Results obtained as exhibited in Fig. 12 show that the lift is dominated by the incidence angle while the thrust is dominated by the flapping angle (other parameters remaining constant).

From the above component-wise force analysis, it can be deduced that also an appropriate combination of these force elements can be obtained to produce optimum lift and thrust. The optimization of this problem is also currently under study.

### 3.1.3 Parametric Study for Bi-Wing

A parametric study is carried out to assess the influence of some flapping wing motion parameters to the flight performance desired. The study considers the following parameters: the effect of flapping frequency and total flapping angle. The results are exhibited in Fig. 13. From this study, in general, the lift (at higher degree of frequency) and thrust forces always increases as the flapping frequency increases. As for the flapping amplitude, the thrust increases but the lift decreases over the cycle.

By referring to Pennycuick's [50] and Tucker's formula [51] to associate wing aspect ratio and wing area of birds, the present ornithopter model operating frequencies as anticipated in Fig. 13 are close to the operating flapping frequency values of selected birds shown in Table 18.

The phase lag angle between the pitching and flapping motion should be in such way that when the relative air velocity is at its peak, the pitch angle should be maximum. With such condition, this can be achieved only if the phase angle

**Table 7:** Average lift and thrust with variation of flapping frequency.

Av. Forces (N)	Frequency, f (Hz)						
	2.96	5	7	9	11	13	15
<b>Lift</b>	0.1536	0.09848	0.06621	0.06189	0.07878	0.1186	0.1785
<b>Thrust</b>	-0.03580	0.02167	0.1110	0.2366	0.3990	0.6031	0.8515

Av. Forces (N)	Flapping Amplitude, $\beta$ (°)						
	20	30	40	50	60	70	80
Lift	0.1976	0.1606	0.1252	0.09623	0.06621	0.03899	0.01668
Thrust	-0.06182	-0.04379	-0.01122	0.04039	0.1110	0.2053	0.3287

**Table 8:** Average lift and thrust with variation of flapping amplitude.

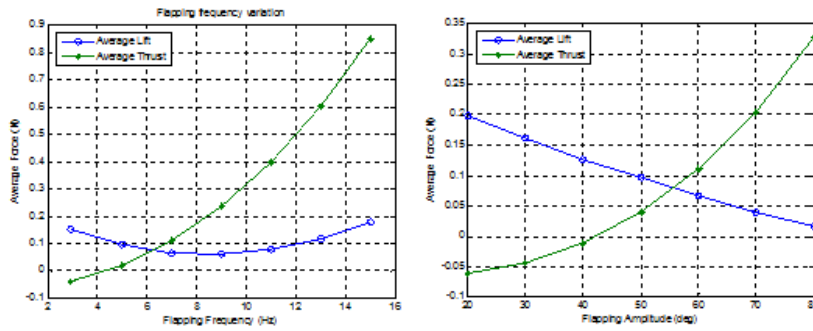


**Figure 13:** Parametric study on the influence of flapping frequency and flapping amplitude on cyclic lift and thrust (bi-wing, semi-elliptical planform).

is  $\pi/2$  (90). Table 9 shows the value for both average values of lift and thrust forces and it is in agreement with the statement above.

### 4 Analysis and Results for Quad-Wing

For the quad-wing kinematics and aerodynamics, the present work takes into account the influence of the fore-wing induced downwash on the hind-wing effective angle of attack. This effect is modeled by assuming that, at any instant, the circulation  $\Gamma$  of the fore-wing acts at its quarter-chord point, and the induced downwash is calculated at the three quarter-chord point of the hind-wing, as depicted in Fig. 16.

Following Kutta-Joukowski Law, the instantaneous equivalent circulation generated by the fore-wing is given by

$$\Gamma = \frac{L_{fore}}{\rho U_{\infty}} \tag{36}$$

and the induced velocity  $V_i$ , following Biot-Savart law is given by

$$V_i = \frac{\Gamma}{2\pi d} \tag{37}$$

Following Fig. 16, for small angle of attack, the induced angle is formulated as

$$\alpha_{induced} \approx \frac{V_i}{U_{\infty}} \tag{38}$$

Therefore the pitching angle of the hind-wing is given by

$$\theta_{hindwing}(t) = \theta_{0hindwing} \cos(\omega t + \phi) - \frac{V_i}{U} + \theta_{fphindwing}$$

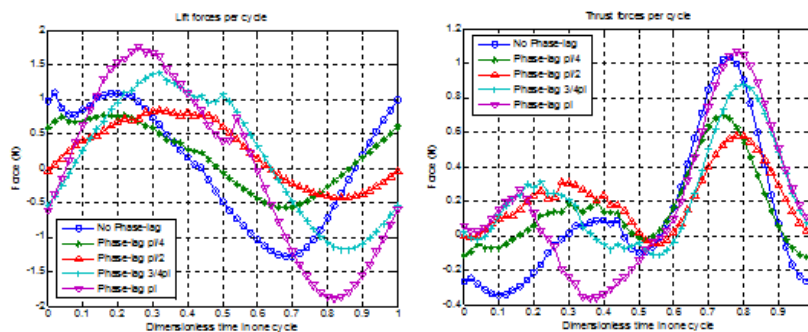


**Figure 14:** Lift and thrust variation with phase lag angle.

**Table 9:** Average lift and thrust variation with lag of phase angle.

Av. Forces (N)	Pitch and Flap phase lag				
	0	$\pi/4$	$\pi/2$	$3\pi/4$	$\pi$
Lift	0.06621	0.1877	0.2289	0.1619	0.005574
Thrust	0.1110	0.1571	0.2063	0.2263	0.1991

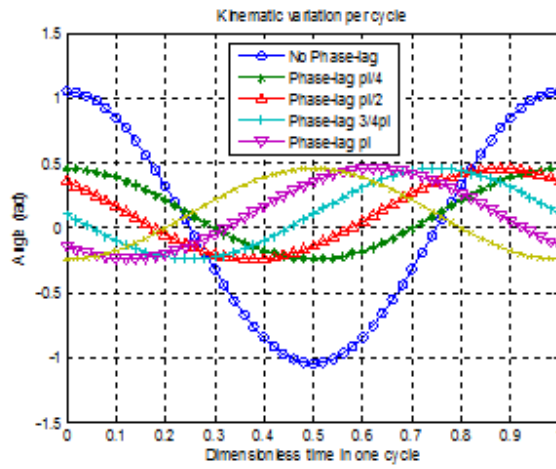


**Figure 15:** Kinematics variation with phase lag angle.

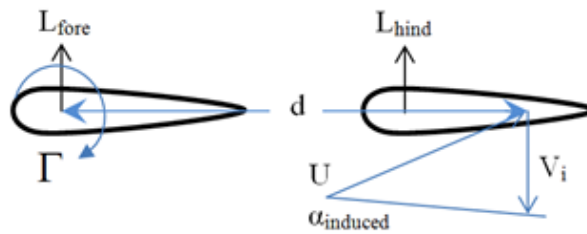


**Figure 16:** Schematic diagram of the fore wing downwash and the induced angle of attack on the hind wing.

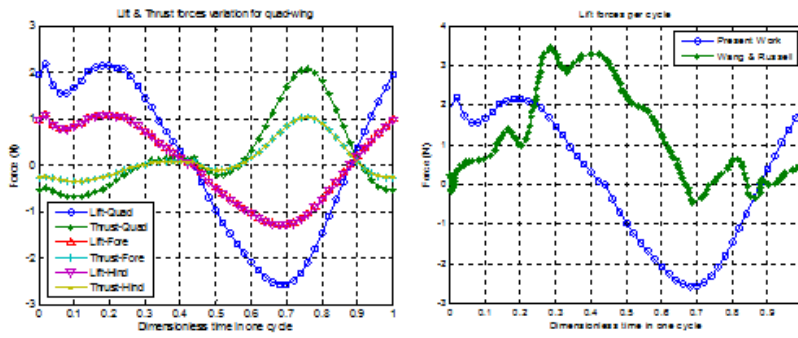


**Figure 17:** Left: Lift and thrust for quad-wing ornithopter; Right: Qualitative investigation with Wang & Russell [20].

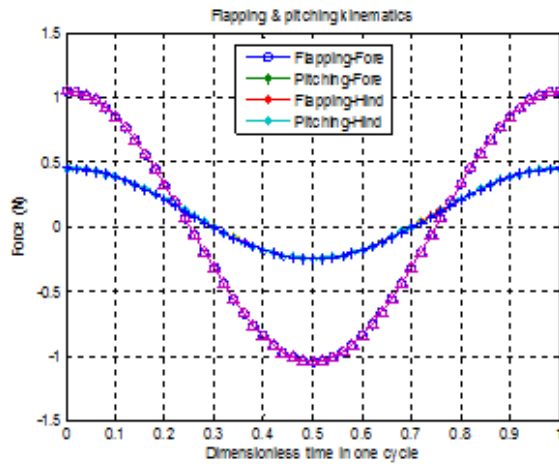


**Figure 18:** Flapping & pitching kinematics for Fore-wing & Hind-wing.

The analysis is then carried out for the quad-wing with similar wing geometry as for the bi-wing. Initial initiative was done with an assumption that the fore- and hind-wings are closely attached; meaning of inexistence of gap between the leading edge of the hind-wing and the trailing edge of the fore-wing. The results for quad-wing configuration below are obtained using the same wing geometry and parameters used in bi-wing case, for fore- (front) wing and hind- (latter) wings. The results are compared and analyzed to appreciate the influence of physical refinements in the computational procedure and for validation purposes. This analysis also accounts for the induced angle of attack on the hind-wing due to downwash of the fore-wing. The results are presented in Figs. 17 and 18, and Table 10.

Fig. 17 compares the lift computed using the present model to Wang and Russell’s more elaborate model calculation [20]. This comparison is very qualitative, for proof of concept considerations. Fig. 18 shows the default motions of flapping and pitching for both fore-wing and hind-wing, which are in cosine function.

#### 4.1 Variation of Oscillatory Articulation of the Quad-Wing

Following the procedure and parametric study carried out for bi-wing ornithopter, the present study also addresses the flapping kinematics accordingly, by taking into considerations what has been learned from bi-wing parametric study. The fore-wing and hind-wing are arranged in tandem without gap, so that the leading edge of the hind-wing touches the trailing edge of the forewing, and they are

Forces (N)	Present Work	Fore-wing	Hind-wing	Ref.[20]
Average Lift	0.1193	0.0662	0.0531	1.136567
Average Thrust	0.2248	0.1110	0.1138	-

**Table 10:** Average lift and thrust for present work.

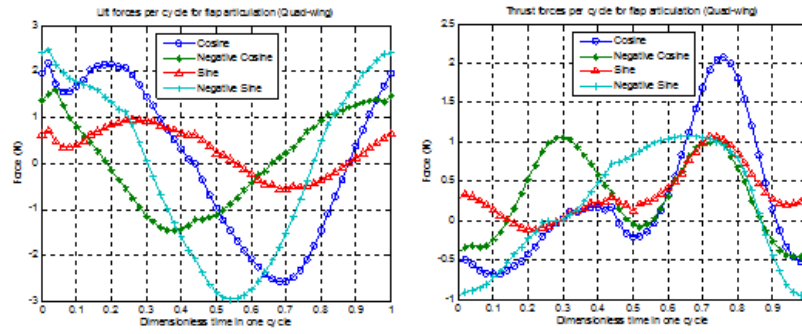


**Figure 19:** Lift and thrust for quad-wing ornithopter for each flapping kinematics definition (pitching motion in cosine function).

**Table 11:** Average lift and thrust for quad-wing ornithopter for each flapping kinematics definition (pitching motion in cosine function).

Av. Forces (N)	Quadwing (Hind-wing Art.) (Fore-wing in cosine function)			
	Cosine	- Cosine	Sine	- Sine
<b>Lift</b>	0.1193	0.0828	0.2719	-0.0376
<b>Thrust</b>	0.2248	0.3103	0.3307	0.1706

moving simultaneously. The flapping and pitching motions of both forewing and hind-wing are varied following negative cosine, sine and negative sine functions. The results, as exhibited in Fig. 19 and Table 11, show that the synchronous (in-phase) sinusoidal pitching and flapping produce the maximum average values of lift and thrust. Table 12 and 13 show the articulation of kinematics in pitching and flapping, for lift and thrust forces respectively. These results also indicate variation of such oscillatory articulation possibilities that could be further tailored to meet certain objectives.

### 4.2 Component-wise Forces for Quad-Wing

Individual contributions of the pitching-flapping motion on the flight performance are assessed. The calculation is performed on semi-elliptical wing. Results obtained as exhibited in Fig. 20 and Table 14 depict similar behavior to the bi-wing cases that the lift is dominated by the incidence angle. For the thrust, the flapping motion has a very dominant influence over the force.

From the component-wise force analysis, it can be summarized that also a suitable combination of these force elements can be attained in order to generate optimum lift and thrust. The optimization of this problem is also currently being studied.

### 4.3 Parametric Study for Quad-Wing

A parametric study is carried out to assess the influence of certain flapping wing motion parameters to the flight performance desired. The study considers the following parameters: the effect of flapping frequency and the gap distance between fore-wing and hind-wing. The results are exhibited in Fig. 21, Table 15 and 16. It can be seen that the effect of flapping frequency exhibits similar trend as bi-wing's. For the gap distance effect, as the distance increases, the lift increases but the thrust decreases in small magnitude.

Results obtained as exhibited in Fig. 22 show the lift produced for various scenarios involving phase combinations between flapping and pitching motions

**Table 12:** Average lift for quad-wing ornithopter for each pitching and flapping kinematics definition.

Av. Lift (N) FLAP (Fore-wing)	FLAP (Hind-wing)			
	Cosine	- Cosine	Sine	- Sine
<b>Cosine</b>	0.1193	0.0828	0.2719	-0.0376
<b>- Cosine</b>	0.0979	0.0605	0.2513	-0.0640
<b>Sine</b>	0.2587	0.2238	0.4045	0.1014
<b>- Sine</b>	-0.0138	-0.0536	0.1452	-0.1762

Av. Thrust (N)	FLAP (Hind-wing)			
FLAP (Fore-wing)	Cosine	- Cosine	Sine	- Sine
Cosine	0.2248	0.3103	0.3307	0.1706
- Cosine	0.3075	0.3924	0.4138	0.2526
Sine	0.3358	0.4238	0.4460	0.2785
- Sine	0.1624	0.2457	0.2625	0.1097

**Table 13:** Average thrust for quad-wing ornithopter for each pitching and flapping kinematics definition.

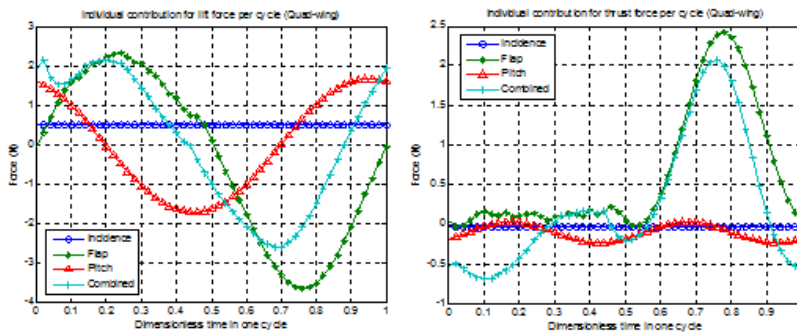


**Figure 20:** Component-wise contribution for quad-wing.

Av. Forces (N)	Individual Contribution for Quad-wing			
	Incidence only	Flap only	Pitch only	Combined
Lift	0.5052	-0.3412	0.0293	0.1193
Thrust	-0.0329	0.6162	-0.1036	0.2248

**Table 14:** Average lift and thrust (quad-wing) for each individual contribution.

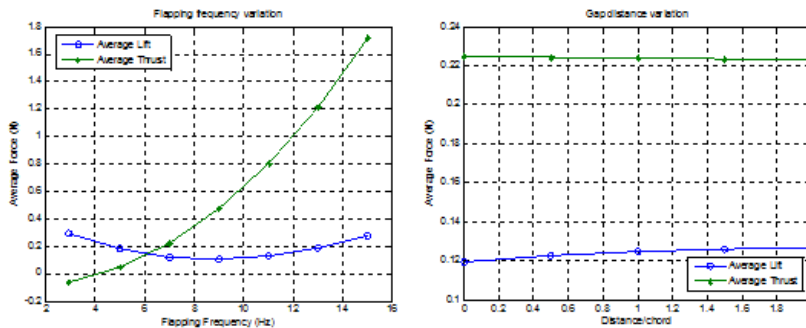


**Figure 21:** Parametric study on the influence of flapping frequency and gap distance between fore-wing and hind-wing on cyclic lift and thrust (quad-wing, semi-elliptical planform).

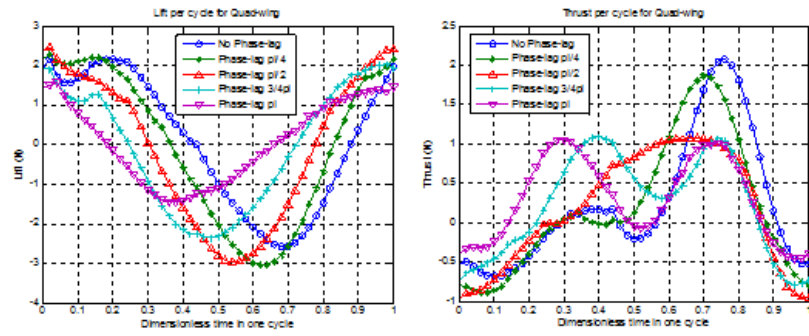


**Figure 22:** Fore flapping phase lag variation for Quad-wing.

**Table 15:** Average lift and thrust with variation of flapping frequency.

Av. Forces (N)	Flapping Freq., $f$ (Hz)						
	2.96	5	7	9	11	13	15
<b>Lift</b>	0.294	0.182	0.119	0.107	0.128	0.187	0.277
<b>Thrust</b>	-0.065	0.047	0.225	0.476	0.802	1.215	1.718

of the individual fore- and hind-wings. Table 17 summarizes the average forces per cycle for the selected scenarios.

A deduction can be made from the results from Table 17 that having in-phase flight produces the maximum lift and thrust, among the others. In conformity with the observation by Deng & Hu [52] and Alexander [53] in their study, the present study also indicates that when quad-wing insect like dragonfly performs aggressive maneuvers, they will employ in-phase flight to generate larger aerodynamic forces. However further analysis to optimize the combination of these parameters is still under progress.

## 5 Comprehensive Assessment of Modeling Results

Better understanding of the production of lift and thrust are intended for current simplified modeling of both bi-wing and quad-wing ornithopters. It is also meant to build a comprehensive foundation and act as a guideline to develop a simple experimental model ornithopter. A more sophisticated computational and experimental prototype can be built in a progressive manner by superposing other significant characteristics. To gain better comprehension into the kinematic and aerodynamic modelling of bi-wing and quad-wing ornithopters, comparison will be made on the basic characteristics and performance of selected ornithopter models with those of selected real birds and insects.

The use of CFD computation to simulate the vorticity field for quad-wing is a complex study as reported by Wang and Russell [20]. Although on average, an upward net force is generated on the wing due to the downward flow created by the wing motion, the computation is not readily related to the computational results for lift and thrust. For future progress, such result could be the basis platform to the present aerodynamics and kinematics modeling of non-deforming quad-wing ornithopter, which can extensively and progressively be further redeveloped and refined to approach the genuine living biosystem flight features, such as those of dragonfly and other related enthomopters.

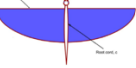
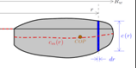
For this purpose, Table 18 has been prepared as an extension of the earlier Table presented in [26], to obtain an insight of the flight characteristics and basic performance of ornithopter and entomopter models, and birds and insect. Table 18 exhibits the ratio of the lift per cycle, thrust per cycle, lift per aspect ratio and

**Table 16:** Average lift and thrust with variation of gap distance (expressed in chords) between fore- and hind-wing.

Av. Forces (N)	Distance, $d$				
	No Gap	$1/2 c$	$1 c$	$1.5 c$	$2 c$
<b>Lift</b>	0.1193	0.1227	0.1247	0.1260	0.1270
<b>Thrust</b>	0.2248	0.2241	0.2237	0.2234	0.2232

Av. Forces (N)	phase lag of fore-wing flapping motion (Fore- & Hind-wing in cosine function)				
	0	$\pi/4$	$\pi/2$	$3\pi/4$	$\pi$
Lift	0.1193	0.0123	-0.0376	-0.0208	0.0847
Thrust	0.2248	0.1792	0.1706	0.2312	0.3107

**Table 17:** Average lift and thrust with variation of flapping phase lag for fore-wing.

ORNITHOPTER MODEL	Present Work (Semi-elliptical)	Previous Work (Semi-elliptical) [26]	Malik & Ahmad [55]	Byl's hummingbird-scale robot [56]	DeLaurier's pterosaur model [11]
Length	-	-	-	-	-
Wingspan	0.4m	0.4m	0.4m	0.16m	5.4864m
Aspect Ratio	6.36	6.36	6.2	-	-
Wing Area	0.0251m <sup>2</sup>	0.0251m <sup>2</sup>	0.0251m <sup>2</sup>	-	-
Lift/Cycle	0.0662N	0.1403N	0.1705N	0.2000N	177.923N
Thrust/Cycle	0.1110N	1.3163N	0.0201N	-	-
					
Lift(N) Wingspan(m)	0.1655N/m	0.351 N/m	0.4263N/m	1.25N/m	32.431N/m
Thrust(N) Wingspan(m)	0.2775N/m	3.291N/m	0.0503N/m	-	-
Wing Loading	2.64N/m <sup>2</sup>	5.59N/m <sup>2</sup>	6.79 N/m <sup>2</sup>	-	-
Lift(N) Aspect Ratio	0.025N	0.022N	0.027N	-	-
BIRD	Wandering Albatross	Turkey Vulture	Red-tailed Hawk	Bald Eagle	Peregrine Falcon
Length	110 cm	67 cm (26 in)	49 cm (19 in)	79 cm (31 in)	46 cm (18 in)
Wingspan	300 cm	171 cm (67 in)	125 cm (49 in)	203 cm (80 in)	116 cm (46 in)
Aspect Ratio	15	7.0	7.1	6.6	8.91
Wing Area	0.643 m <sup>2</sup>	0.612 m <sup>2</sup>	0.188 m <sup>2</sup>	0.703 m <sup>2</sup>	0.151 m <sup>2</sup>
Weight	9.00 kg	1.8 kg (4 lb)	1.082 kg (2.4 lb)	4.3 kg (9.5 lb)	0.952kg (2.1 lb)
					
Lift(N) Wingspan(m)	29.4N/m	10.5N/m	8.656N/m	21.182N/m	8.206N/m
Wing Loading	137.31 N/m <sup>2</sup>	28.84 N/m <sup>2</sup>	57.41 N/m <sup>2</sup>	60.00 N/m <sup>2</sup>	61.80 N/m <sup>2</sup>
Lift(N) Aspect Ratio	5.87 N	2.57 N	1.52 N	6.52 N	1.07 N

\*For the ornithopter models, the lift used in the calculation is the Lift/Cycle whereas for the birds, the lift represents the weight of the birds

**Table 18:** Comparison of basic performance of ornithopter models and birds (extended from earlier work [25, 26, 54]).

the wing loading calculated using the present simplified computational model and those obtained by other investigators; for comparison, the weight per wingspan of a selected sample of birds are also exhibited. Although the comparison is by no means rigorous, it may shed some light on how the geometrical modelling and the flapping motion considered in the computational model may contribute to the total lift produced and how further refinement could be synthesized.

The development carried out in this work is addressed to biomimicry of biosystem flying in the Reynolds number range of  $1.0 \times 10^4$  to  $1.0 \times 10^5$  which is turbulent. The projected ornithopter and MAV will be also operating in this range of Reynolds number. The aerodynamics that have been adopted in the present work takes into account viscous correction appropriately (DeLaurier [11], Shyy et al. [7]). Shyy et al [7] show that for all airfoils, the CL/CD ratio exhibits a clear Reynolds number dependency. For Re varying between  $7.5 \times 10^4$  and  $2.0 \times 10^6$ , CL/CD changes by a factor of 2 to 3 for the airfoils tested.

In the present work, viscosity effects are taken into account following the approach and results of DeLaurier [11], using the computational formulation as given in the present paper as a simplified approach to the problem, but validated through comparison with comparable experimental results range. Such approach can be justified as a preliminary step towards more accurate approach and to develop simple flapping ornithopter MAV.

## 6 Conclusions

The present work has been performed to assess the effect of flapping-pitching motion with pitch-flap phase lag in the flight of ornithopter. In this conjunction, a computational model has been considered, and a generic computational

method has been adopted, utilizing strip theory and two-dimensional unsteady aerodynamic theory of Theodorsen with modifications to account for three-dimensional and viscous effects and leading edge suction. The study is carried out on semi-elliptical wing planforms. The results have been compared and validated with other literatures within similar unsteady aerodynamic approach and general physical data, and within the physical assumptions limitations; encouraging qualitative agreements or better have been indicated, which meet the proof of concept objectives of the present work. For the bi-wing flapping ornithopter, judging from lift per unit span, the present flapping-wing model performance is comparable to those studied by Yu et al [47]. The analysis and simulation by splitting the flapping and pitching motion shows that: (a) The lift is dominantly produced by the incidence angle (b) The thrust is dominated by flapping motion (c) Phase-lag could be utilized to obtain optimum lift and thrust for each wing configurations.

For the quad-wing ornithopter, at the present stage, the simplified computational model adopted verified the gain in lift obtained as compared to bi-wing flapping ornithopter, in particular by the possibility of varying the phase lag between the flapping and pitching motion of individual wing as well as between the fore- and hind-wings. A structured approach has been followed to assess the effect of different design parameters on lift and thrust of an ornithopter, as well as the individual contribution of the component of motion. These results lend support to the utilization of the generic modelling adopted in the synthesis of a flight model, although more refined approach should be developed. Various physical elements could be considered to develop ornithopter kinematic and aerodynamic modelling, as well as using more refined aerodynamic computation, such as CFD or lifting surface methods. In retrospect, a generic physical and computational model based on simple kinematics and basic aerodynamics of a flapping-wing ornithopter has been demonstrated to be capable of revealing its basic characteristics and can be utilized for further development of a flapping-wing MAV. Application of the present kinematic, aerodynamic and computational approaches shed some light on some of the salient aerodynamic performance of the quad-wing ornithopter.

## Acknowledgements

The authors would like to thank University Putra Malaysia (UPM) for granting Research University Grant Scheme (RUGS) Project Code: 9378200, under which the present research is carried out.

## References

- [1] S. Ho, H. Nassef, N. Pornsinsirirak, Y.-C. Tai, and C.-M. Ho. Unsteady Aerodynamics and Flow Control for Flapping Wing Flyers. *Progress in Aerospace Sciences* 39: 635–681, 2003.
- [2] T. Weis-Fogh. Quick Estimates of Flight Fitness in Hovering Animals, Including Novel Mechanisms for Lift Production. *Journal of Experimental Biology* 5: 169–230, 1973.
- [3] C. P. Ellington. The Aerodynamics of Hovering Insect Flight, III. Kinematics. *Phil. Trans. R. Soc. London B* 305: 41-78, 1984.
- [4] C. P. Ellington. The Novel Aerodynamics of Insect Flight: Applications to Micro-Air Vehicles. *Journal of Experimental Biology* 202: 3439–3448, 1999.
- [5] C. P. Ellington. The Aerodynamics of Hovering Insect Flight, I, Quasi-Steady Analysis. *Phil. Trans. R. Soc. London B* 305: 1-15, 1984.

- [6] W. Shyy, M. Berg, and D. Ljungqvist. Flapping and Flexible Wings for Biological and Micro Air Vehicles. *Progress in Aerospace Sciences* 35: 455-505, 1999.
- [7] W. Shyy, H. Aono, S. K. Chimakurthi, P. Trizila, C.-K. Kang, C. E. S. Cesnik, and H. Li. Recent Progress in Flapping Wing Aerodynamics and Aeroelasticity. *Progress in Aerospace Science* 46(7), 284-327, 2010.
- [8] M. H. Dickinson, F.-O. Lehmann, and S. P. Sane. Wing Rotation and the Aerodynamic Basis of Insect Flight. *Science* 284(5422): 1954-1960, 1999.
- [9] R. Zbikowski. On Aerodynamic Modelling of an Insect-like Flapping Wing in hover for Micro Air Vehicles. *Phil. Trans. R. Soc. London A* 360: 273-290, 2002.
- [10] S. A. Ansari, R. Zbikowski, K. Knowles. Aerodynamic Modelling of Insect-like Flapping Flight for Micro Air Vehicles. *Progress in Aerospace Sciences* 42: 129-172, 2006.
- [11] J. D. DeLaurier. An Aerodynamic Model for Flapping Wing Flight. *Aeronautical Journal of the Royal Aeronautical Society* 97: 125-130, 1993.
- [12] Z. J. Wang. The Role of Drag in Insect Hovering. *Journal of Experimental Biology* 207: 4147- 4155, 2004.
- [13] Z. J. Wang. Dissecting Insect Flight. *Annu. Rev. Fluid Mech.* 37: 183-210, 2005.
- [14] N. C. Rosenfeld. An Analytical Investigation of Flapping Wing Structures for MAV. Ph.D. Thesis, University of Maryland, 2011.
- [15] B. Nicholson, S. Page, H. Dong, and J. Slater. Design of a Flapping Quad-Winged Micro Air Vehicle. AIAA-4337, 2007.
- [16] W. J. Maybury, and F.-O. Lehmann. The Fluid Dynamics of Flight Control by Kinematic Phase Lag Variation Between Two Robotic Insect Wings. *Journal of Experimental Biology* 207: 4707-4726, 2004.
- [17] J. Ratti. QV-The Quad Winged, Energy Efficient, Six Degree of Freedom Capable Micro Air Vehicle. PhD Thesis, Georgia Institute of Technology, 2011.
- [18] D. T. Prosser. Flapping Wing Design for a Dragon-fly like MAV. M.Sc. Thesis, Rochester Institute of Technology, 2011.
- [19] K. A. Strang. Efficient Flapping Flight of Pterosaurs. PhD Thesis, Stanford University, 2009.
- [20] Z. J. Wang, and D. Russell. Effect of Forewing and Hindwing Interactions on Aerodynamic Forces and Power in Hovering Dragonfly Flight. *Physical Review Letters* 99(148101), 2007.
- [21] H. E. Taha, M. R. Hajj, and A. H. Nayfeh. Flight Dynamics and Control of Flapping Wing MAV - A Review. *Nonlinear Dynamics* 70: 907-939, 2012.
- [22] H. E. Taha, M. R. Hajj, and P. S. Beran. State-Space Representation of the Unsteady Aerodynamics of Flapping Flight. *Aerospace Science & Technology* 34: 1-11, 2014.
- [23] U. M. Norberg. Hovering Flight of *Plecotusauritus*, L. *Bijdr. Dierk* 40, 62-66 (Proc.2<sup>nd</sup> int. Bat. Res. Conf.), 1970.

- [24] R. Tedrake, Z. Jackowski, R. Cory, J. W. Roberts, and W. Hoberg. Learning to Fly like a Bird. *Communications of the ACM*, 2009.
- [25] H. Djojodihardjo, A. S. S. Ramli, and S. Wiriadidjaja. Kinematic and Aerodynamic Modeling of Flapping Wing Ornithopter. *Procedia Engineering (Elsevier)* 50: 848-863, 2012.
- [26] H. Djojodihardjo, and A. S. S. Ramli. Kinematic and Unsteady Aerodynamic Modelling, Numerical Simulation and Parametric Study Of Flapping Wing Ornithopter. *Proceedings, International Forum on Aeroelasticity and Structural Dynamics, Bristol*, 2013.
- [27] A. R. Jones, N. A. Bakhtian, and H. Babinsky. Low Reynolds Number Aerodynamics of Leading-edge Flaps. *Journal of Aircraft* 45(1): 342-345, 2008.
- [28] H. Djojodihardjo, and M. A. A. Bari. Kinematic and Unsteady Aerodynamic Modelling of Flapping Bi- and Quad-Wing Ornithopter. *Proceedings-ICAS 2014, Paper 2014-0433*, 2014.
- [29] T. Theodorsen. General Theory of Aerodynamic Instability and the Mechanism of Flutter. *NACA Report No.496*, 1935.
- [30] R. T. Jones. The Unsteady Lift of a Wing of Finite Aspect Ratio. *NACA Report No.681*, 1940.
- [31] E. C. Polhamus. A Concept of the Vortex Lift of Sharp-Edge Delta Wings Based On A Leading-Edge-Suction Analogy. *NASA TN D-3767*, 1966.
- [32] E. C. Polhamus. Application of the Leading-Edge-Suction Analogy Of Vortex Lift To The Drag Due To Lift Of Sharp-Edge Delta Wings. *NASA TN D-4739*, 1968.
- [33] H. Ashley, M. T. Landahl, and S. E. Widnall. New Directions in Lifting Surface Theory. *AIAA Journal* 3(1), 1965.
- [34] A. Albano, and W. P. Rodden. A Doublet-Lattice Method for Calculating Lift Distributions on Oscillating Surfaces in Subsonic Flows. *AIAA Journal* 7(2): 279-285, 1969.
- [35] R. H. Djojodihardjo, and S. E. Widnall. A Numerical Method for the Calculation of Nonlinear, Unsteady Lifting Potential Flow Problems. *AIAA Journal* 7(10): 2001-2009, 1969.
- [36] J. Murua, R. Palacios, and J. M. R. Graham. Applications of the Unsteady Vortex-Lattice Method in Aircraft Aeroelasticity and Flight Dynamics. *Progress in Aerospace Sciences* 55: 46-72, 2012.
- [37] H. Djojodihardjo, A. S. S. Ramli, and S. Wiriadidjaja. Generic Modelling and Parametric Study of the Aerodynamic Characteristics of Flapping Wing Micro-Air-Vehicle. *Applied Mech. and Materials* 225: 18-25, 2012.
- [38] H. Djojodihardjo, M. A. A. Bari, A. S. M. Rafie, and S. Wiriadidjaja. Further Development of the Kinematic and Aerodynamic Modeling and Analysis of Flapping Wing Ornithopter from Basic Principles. *Applied Mech. and Materials* 629: 9-17, 2014.
- [39] R. L. Harmon. Aerodynamic Modelling of a Flapping Membrane Wing Using Motion Tracking Experiments. *M.Sc. Thesis, University of Maryland*, 2008.
- [40] J. O. Scherer. Experimental and Theoretical Investigation of Large Amplitude Oscillating Foil Propulsion Systems. *Hydronautics, Laurel, Md*, 1968.

- [41] H. Multhopp. Methods for Calculating the Lift Distribution of Wings (Subsonic Lifting-Surface Theory). ARC R&M No.2884, 1955.
- [42] I. E. Garrick. Propulsion of a Flapping and Oscillating Aerofoil. NACA Report No.567, 1936.
- [43] I. E. Garrick. On Some Reciprocal Relations in the Theory of Nonstationary Flows. NACA Report No.629, 1938.
- [44] A. M. Kuethe, and C.-Y. Chow. The Finite Wing, Foundations of Aerodynamics. Fourth edition, John Wiley, New York: 145-164, 1986.
- [45] J. D. Anderson. Fundamentals of Aerodynamics. Fourth edition, McGraw-Hill, New York, 2004.
- [46] M. Y. Zakaria, H. E. Taha, M. R. Hajj. Shape and Kinematic Design Optimization of Pterosaur Replica. AIAA 2014-2869, 2014.
- [47] C. Yu, D. Kim, and Y. Zhao. Lift and Thrust Characteristics of Flapping Wing Aerial Vehicle with Pitching and Flapping Motion. Journal of Applied Mathematics and Physics 2: 1031-1038, 2014.
- [48] T. Fujiwara, K. Hirakawa, S. Okuma, T. Udagawa, S. Nakano, and K. Kikuchi. Development of a Small Flapping Robot: Motion Analysis During Takeoff by Numerical Simulation and Experiment. Mechanical Systems and Signal Processing 22(6): 1304-1315, 2008.
- [49] M. W. Chen, Y. L. Zhang, and M. Sun. Wing and Body Motion and Aerodynamic and Leg Forces During Take-off in Droneflies. Journal of the Royal Society Interface 10, 2013.
- [50] C. J. Pennycuik. Predicting Wingbeat Frequency and Wavelength of Birds. Journal of Experimental Biology 150: 171-185, 1990.
- [51] V. A. Tucker. Gliding Birds: The Effect of Variable Wing Span. J. Exp. Biology 133, 1987.
- [52] X. Deng, and Z. Hu. Wing-wing Interactions in Dragonfly Flight. A Publication of Ine-Web.Org, 10.2417/1200811.1269, 2008.
- [53] D. E. Alexander. Unusual Phase Relationships between the Forewings and Hindwings in Flying Dragonflies. J. Exp. Biology 109: 379-383, 1984.
- [54] H. Djojodihardjo, A. S. S. Ramli, M. S. A. Aziz, and K. A. Ahmad. Numerical Modelling, Simulation and Visualization of Flapping Wing Ornithopter. Keynote Address, International Conference on Engineering Materials and Processes (ICEMAP), Chennai, 2013.
- [55] M. A. Malik, and F. Ahmad. Effect of Different Design Parameters on Lift, Thrust, and Drag of an Ornithopter. Proceedings of the World Congress on Engineering 2010 Vol. II, London, U.K., 2010.
- [56] K. Byl. A Passive Dynamic Approach for Flapping Wing Micro Aerial Vehicle Control. ASME Dynamic Systems and Controls Conference, 2010.